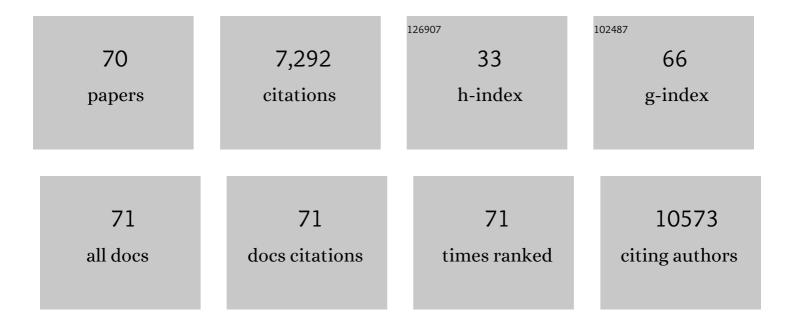
Timothy L Kelly

List of Publications by Year in descending order

Source: https://exaly.com/author-pdf/3787587/publications.pdf Version: 2024-02-01



#	Article	IF	CITATIONS
1	Perovskite solar cells with a planar heterojunction structure prepared using room-temperature solution processing techniques. Nature Photonics, 2014, 8, 133-138.	31.4	2,425
2	Investigation of CH ₃ NH ₃ PbI ₃ Degradation Rates and Mechanisms in Controlled Humidity Environments Using <i>in Situ</i> Techniques. ACS Nano, 2015, 9, 1955-1963.	14.6	1,171
3	Origin of the Thermal Instability in CH ₃ NH ₃ PbI ₃ Thin Films Deposited on ZnO. Chemistry of Materials, 2015, 27, 4229-4236.	6.7	548
4	Compact Layer Free Perovskite Solar Cells with 13.5% Efficiency. Journal of the American Chemical Society, 2014, 136, 17116-17122.	13.7	407
5	Effect of CH ₃ NH ₃ PbI ₃ thickness on device efficiency in planar heterojunction perovskite solar cells. Journal of Materials Chemistry A, 2014, 2, 19873-19881.	10.3	314
6	In situ studies of the degradation mechanisms of perovskite solar cells. EcoMat, 2020, 2, e12025.	11.9	123
7	Decomposition and Cell Failure Mechanisms in Lead Halide Perovskite Solar Cells. Inorganic Chemistry, 2017, 56, 92-101.	4.0	117
8	Effect of relative humidity on crystal growth, device performance and hysteresis in planar heterojunction perovskite solar cells. Nanoscale, 2016, 8, 6300-6307.	5.6	113
9	Plasmonic Enhancement of Dye Sensitized Solar Cells in the Red-to-near-Infrared Region using Triangular Core–Shell Ag@SiO ₂ Nanoparticles. ACS Applied Materials & Interfaces, 2013, 5, 11044-11051.	8.0	102
10	Fatigue resistance of a flexible, efficient, and metal oxide-free perovskite solar cell. Journal of Materials Chemistry A, 2015, 3, 9241-9248.	10.3	100
11	Dopant-free molecular hole transport material that mediates a 20% power conversion efficiency in a perovskite solar cell. Energy and Environmental Science, 2019, 12, 3502-3507.	30.8	90
12	Template approaches to conjugated polymer micro- and nanoparticles. Chemical Society Reviews, 2010, 39, 1526.	38.1	79
13	Photon Upconversion by Triplet–Triplet Annihilation in Ru(bpy) ₃ - and DPA-Functionalized Polymers. Journal of Physical Chemistry Letters, 2013, 4, 4113-4118.	4.6	79
14	Supercapacitive Properties of PEDOT and Carbon Colloidal Microspheres. ACS Applied Materials & Interfaces, 2009, 1, 2536-2543.	8.0	77
15	Highly Stable Porous Silicon–Carbon Composites as Label-Free Optical Biosensors. ACS Nano, 2012, 6, 10546-10554.	14.6	76
16	Self-assembled polymetallic square grids ([2 × 2] M4, [3 × 3] M9) and trigonal bipyramidal clusters (M5)—structural and magnetic properties. Journal of Materials Chemistry, 2006, 16, 2645-2659.	6.7	71
17	Supramolecular â€~flat' Mn9grid complexes—towards functional molecular platforms. Dalton Transactions, 2006, , 2835-2851.	3.3	66
18	Self-Assembled Dinuclear, Trinuclear, Tetranuclear, Pentanuclear, and Octanuclear Ni(II) Complexes of a Series of Polytopic Diazine Based Ligands:Â Structural and Magnetic Properties. Inorganic Chemistry, 2003, 42, 2950-2959	4.0	59

TIMOTHY L KELLY

#	Article	IF	CITATIONS
19	Supramolecular Mn(II) and Mn(II)/Mn(III) Grid Complexes with [Mn9(μ2-O)12] Core Structures. Structural, Magnetic, and Redox Properties and Surface Studies. Inorganic Chemistry, 2004, 43, 3812-3824.	4.0	56
20	Chemical stability and degradation mechanisms of triangular Ag, Ag@Au, and Au nanoprisms. Physical Chemistry Chemical Physics, 2014, 16, 12407-12414.	2.8	55
21	Carbon and Carbon/Silicon Composites Templated in Rugate Filters for the Adsorption and Detection of Organic Vapors. Advanced Materials, 2011, 23, 1776-1781.	21.0	54
22	Identification and Quantification of Organic Vapors by Time-Resolved Diffusion in Stacked Mesoporous Photonic Crystals. Nano Letters, 2011, 11, 3169-3173.	9.1	52
23	Effect of Acceptor Unit Length and Planarity on the Optoelectronic Properties of Isoindigo–Thiophene Donor–Acceptor Polymers. Chemistry of Materials, 2018, 30, 4864-4873.	6.7	48
24	Copper(II) Complexes of a Series of Alkoxy Diazine Ligands:Â Mononuclear, Dinuclear, and Tetranuclear Examples with Structural, Magnetic, and DFT Studies. Inorganic Chemistry, 2004, 43, 4278-4288.	4.0	47
25	Comparing the Effect of Mesoporous and Planar Metal Oxides on the Stability of Methylammonium Lead Iodide Thin Films. Chemistry of Materials, 2016, 28, 7344-7352.	6.7	45
26	Improving the moisture stability of perovskite solar cells by using PMMA/P3HT based hole-transport layers. Materials Chemistry Frontiers, 2018, 2, 81-89.	5.9	43
27	Mechanism of Shape Evolution in Ag Nanoprisms Stabilized by Thiol-Terminated Poly(ethylene glycol): An in Situ Kinetic Study. Chemistry of Materials, 2013, 25, 4206-4214.	6.7	40
28	Plasmon-Enhanced Triplet–Triplet Annihilation Using Silver Nanoplates. Journal of Physical Chemistry C, 2014, 118, 6398-6404.	3.1	40
29	Mixed Valence Mn(II)/Mn(III) [3 × 3] Grid Complexes: Structural, Electrochemical, Spectroscopic, and Magnetic Properties. Inorganic Chemistry, 2004, 43, 7605-7616.	4.0	39
30	Bisisoindigo: using a ring-fusion approach to extend the conjugation length of isoindigo. Journal of Materials Chemistry A, 2016, 4, 6940-6945.	10.3	39
31	Coordination "Oligomers―in Self-Assembly Reactions of Some "Tritopic―Picolinic Dihydrazone LigandsMononuclear, Dinuclear, Hexanuclear, Heptanuclear, and Nonanuclear Examples. Inorganic Chemistry, 2008, 47, 176-189.	4.0	38
32	Improving the stability and decreasing the trap state density of mixed-cation perovskite solar cells through compositional engineering. Sustainable Energy and Fuels, 2018, 2, 1332-1341.	4.9	36
33	Monodisperse Poly(3,4â€ethylenedioxythiophene)–Silica Microspheres: Synthesis and Assembly into Crystalline Colloidal Arrays. Advanced Materials, 2008, 20, 2616-2621.	21.0	35
34	Panchromatic Enhancement of Light-Harvesting Efficiency in Dye-Sensitized Solar Cells Using Thermally Annealed Au@SiO ₂ Triangular Nanoprisms. Langmuir, 2014, 30, 14352-14359.	3.5	32
35	Elucidating the Failure Mechanisms of Perovskite Solar Cells in Humid Environments Using In Situ Grazing-Incidence Wide-Angle X-ray Scattering. ACS Energy Letters, 2018, 3, 2127-2133.	17.4	32
36	Enhanced Optical Properties and Opaline Selfâ€Assembly of PPV Encapsulated in Mesoporous Silica Spheres. Advanced Functional Materials, 2009, 19, 3737-3745.	14.9	30

TIMOTHY L KELLY

#	Article	IF	CITATIONS
37	Self-Cleaning Organic Vapor Sensor Based on a Nanoporous TiO2 Interferometer. ACS Applied Materials & Interfaces, 2012, 4, 4177-4183.	8.0	30
38	Effect of Molybdenum Oxide Electronic Structure on Organic Photovoltaic Device Performance: An X-ray Absorption Spectroscopy Study. Journal of Physical Chemistry C, 2014, 118, 27735-27741.	3.1	30
39	Recent Advances in Isoindigoâ€Inspired Organic Semiconductors. Chemical Record, 2019, 19, 973-988.	5.8	30
40	Compositional Engineering To Improve the Stability of Lead Halide Perovskites: A Comparative Study of Cationic and Anionic Dopants. ACS Applied Energy Materials, 2018, 1, 181-190.	5.1	29
41	Thin-Film Engineering of Solution-Processable n-Type Silicon Phthalocyanines for Organic Thin-Film Transistors. ACS Applied Materials & amp; Interfaces, 2021, 13, 1008-1020.	8.0	29
42	The Mixed-Valent Manganese [3 × 3] Grid [Mn(III)4Mn(II)5(2poap-2H)6](ClO4)10·10H2O, a Mesoscopic Spin-1/2 Cluster. Inorganic Chemistry, 2006, 45, 3295-3300.	4.0	27
43	7-Azaisoindigo as a new electron deficient component of small molecule chromophores for organic solar cells. Journal of Materials Chemistry A, 2014, 2, 1085-1092.	10.3	27
44	Influence of Surface Morphology on the Colloidal and Electronic Behavior of Conjugated Polymerâ^'Silica Microspheres. Langmuir, 2008, 24, 9809-9815.	3.5	26
45	Carbohydrate-Labeled Fluorescent Microparticles and Their Binding to Lectins. Bioconjugate Chemistry, 2006, 17, 575-578.	3.6	25
46	Complexes derived from hydrolytically â€~unstable' hydrazone ligands – Some unexpected products. Polyhedron, 2005, 24, 807-821.	2.2	22
47	Thermal degradation mechanism of triangular Ag@SiO ₂ nanoparticles. Dalton Transactions, 2016, 45, 9827-9834.	3.3	22
48	Synthesis of Poly(bisisoindigo) Using a Metal-Free Aldol Polymerization for Thin-Film Transistor Applications. ACS Applied Materials & Interfaces, 2020, 12, 14265-14271.	8.0	20
49	Lewis Acid–Base Chemistry of 7-Azaisoindigo-Based Organic Semiconductors. ACS Applied Materials & Interfaces, 2017, 9, 24788-24796.	8.0	19
50	Phase Transfer of Triangular Silver Nanoprisms from Aqueous to Organic Solvent by an Amide Coupling Reaction. Langmuir, 2013, 29, 7052-7060.	3.5	17
51	Soldering Grain Boundaries Yields Inverted Perovskite Solar Cells with Enhanced Open ircuit Voltages. Advanced Materials Interfaces, 2019, 6, 1900474.	3.7	17
52	Effect of Cross-Conjugation on Derivatives of Benzoisoindigo, an Isoindigo Analogue with an Extended π-System. Journal of Physical Chemistry C, 2017, 121, 9110-9119.	3.1	15
53	Heteroatoms as Rotational Blocking Groups for Non-Fullerene Acceptors in Indoor Organic Solar Cells. ACS Energy Letters, 2022, 7, 1635-1641.	17.4	15
54	Improving the rates of Pd-catalyzed reactions by exciting the surface plasmons of AuPd bimetallic nanotriangles. RSC Advances, 2017, 7, 40218-40226.	3.6	14

TIMOTHY L KELLY

#	Article	IF	CITATIONS
55	Nanoscale Control over Phase Separation in Conjugated Polymer Blends Using Mesoporous Silica Spheres. Langmuir, 2010, 26, 421-431.	3.5	12
56	Control and Characterization of Organic Solar Cell Morphology Through Variable-Pressure Solvent Vapor Annealing. ACS Applied Energy Materials, 0, , .	5.1	12
57	Direct conversion X-ray detectors with 70 pA cm ^{â^'2} dark currents coated from an alcohol-based perovskite ink. Journal of Materials Chemistry C, 2022, 10, 1228-1235.	5.5	12
58	Bisisoindigo–Benzothiadiazole Copolymers: Materials for Ambipolar and n-Channel OTFTs with Low Threshold Voltages. ACS Applied Electronic Materials, 2020, 2, 2039-2048.	4.3	11
59	Effect of Molecular Shape on the Properties of Non-Fullerene Acceptors: Contrasting Calamitic Versus 3D Design Principles. ACS Applied Energy Materials, 2018, 1, 6513-6523.	5.1	10
60	Watching Paint Dry: Operando Solvent Vapor Annealing of Organic Solar Cells. Journal of Physical Chemistry Letters, 2020, 11, 6450-6455.	4.6	10
61	Hydrophobic polythiophene hole-transport layers to address the moisture-induced decomposition problem of perovskite solar cells. Canadian Journal of Chemistry, 2019, 97, 435-441.	1.1	8
62	Regioisomerically Pure 1,7-Dicyanoperylene Diimide Dimer for Charge Extraction from Donors with High Electron Affinities. ACS Omega, 2020, 5, 16547-16555.	3.5	6
63	Changes in Optimal Ternary Additive Loading when Processing Large Area Organic Photovoltaics by Spin―versus Bladeâ€Coating Methods. Solar Rrl, 2021, 5, 2100432.	5.8	6
64	Physical supercritical fluid deposition of polymer films: controlling the crystallinity with pressure. Materials Chemistry Frontiers, 2021, 5, 1428-1437.	5.9	5
65	The role of solvent additive in polymer crystallinity during physical supercritical fluid deposition. New Journal of Chemistry, 2021, 45, 11786-11796.	2.8	3
66	Carbon Nanofiber Photonic Crystals: Carbon and Carbon/Silicon Composites Templated in Rugate Filters for the Adsorption and Detection of Organic Vapors (Adv. Mater. 15/2011). Advanced Materials, 2011, 23, 1688-1688.	21.0	2
67	An unusual self-assembling columnar mesogen prepared by tethering a planar naphthalenediimide acceptor to bent phenothiazine donors. Materials Advances, 2022, 3, 328-336.	5.4	2
68	Self-assembly of PBTTTâ \in "C14 thin films in supercritical fluids. Materials Advances, 0, , .	5.4	1
69	Carbohydrate-Labeled Fluorescent Micro-particles And Their Binding To Lectins. Bioconjugate Chemistry, 2007, 18, 1015-1015.	3.6	0
70	Changes in Optimal Ternary Additive Loading when Processing Large Area Organic Photovoltaics by Spin―versus Bladeâ€Coating Methods. Solar Rrl, 2021, 5, 2170104.	5.8	0